New Journal of Physics
The open-access journal for physics

Gold nanorods and nanospheroids for enhancing spontaneous emission

A Mohammadi[1], **V Sandoghdar**[2] **and M Agio**[2,3]

[1] Department of Physics, Persian Gulf University, 75196 Bushehr, Iran
[2] Laboratory of Physical Chemistry, ETH Zurich, 8093 Zurich, Switzerland
E-mail: mario.agio@phys.chem.ethz.ch

New Journal of Physics **10** (2008) 105015 (14pp)
Received 6 June 2008
Published 28 October 2008
Online at http://www.njp.org/
doi:10.1088/1367-2630/10/10/105015

Abstract. We compute the radiative decay rate and the quantum efficiency for an emitter coupled to gold nanorods and nanospheroids using the body-of-revolution finite-difference time-domain method. We study these quantities as a function of the nanoparticle aspect ratio and volume, showing that large enhancements can be achieved with realistic parameters. Moreover, we find that nanospheroids exhibit better performances than nanorods for applications in the visible and near-infrared spectral range.

Contents

[3] Author to whom any correspondence should be addressed.

1. Introduction

The electric field enhancement near rough metal surfaces and metal nanoparticles has been extensively studied in the context of field-enhanced spectroscopy [1, 2]. Recently, the progress in nano-optics has made possible the investigation of configurations where a single molecule is at a controlled distance from a gold nanoparticle [3, 4]. Under appropriate conditions this nanoscopic object can act as an *nanoantenna*, in the sense that it channels the excitation light to the molecule and extracts its fluorescence to the far field more efficiently than if the emitter were in free space [5]. The required electromagnetic resonance that establishes these properties is the localized plasmon mode, which can be spectrally tuned in the visible and near-infrared range by choice of the material, shape and size [6]. The amplitude and polarization of the electromagnetic field near the nanoparticle are very strongly distance-dependent. The matter is further complicated, however, because at distances close to the metallic object fluorescence can be quenched [7, 8]. Several theoretical [8]–[13] and experimental [14]–[20] efforts have studied various aspects of the radiative properties of emitters coupled to nanoantennas. Other types of plasmonic structures such as metal nanowires are also currently being investigated for controlling light–matter interaction [21, 22]. In our laboratory, we have succeeded in separating the effects of excitation enhancement, spontaneous emission modification, and nonradiative decay of a single molecule interacting with a single gold nanoparticle [4, 23].

For weak excitation the fluorescence signal S_o is proportional to $\xi\eta_o|\mathbf{d}\cdot\mathbf{E}_o|^2$, where ξ is the collection efficiency, $\mathbf{d}$ is the dipole moment, $\mathbf{E}_o$ is the electric field at the position of the emitter, and $\eta_o = \Gamma^o_{rad}/(\Gamma^o_{rad}+\Gamma^o_{nrad})$ is the quantum efficiency, where Γ^o_{rad} and Γ^o_{nrad} stand for the radiative and nonradiative decay rates, respectively [4]. Assuming that the collection efficiency does not change when the emitter is coupled to the nanoantenna, the signal enhancement can be written as

$$\frac{S}{S_o} = \frac{\eta}{\eta_o}\frac{|\mathbf{d}\cdot\mathbf{E}|^2}{|\mathbf{d}\cdot\mathbf{E}_o|^2}, \tag{1}$$

where $\mathbf{E}$ is the new local electric field. The modified quantum efficiency η is related to η_o and the radiative decay rate enhancement (Purcell factor) F by [24]

$$\eta = \frac{\eta_o}{(1-\eta_o)/F + \eta_o/\eta_a}, \tag{2}$$

where the antenna efficiency η_a is the fraction of the molecular fluorescence that is not dissipated by the nanoantenna into metal losses [8, 24]. Equation (2) presents two limiting cases. For $\eta_o = 1$, $\eta = \eta_a$ irrespective of F. Because η_a is always less than one, the quantum efficiency can only be reduced. However, the fluorescence signal S can still be enhanced if η_a is not too small and $\mathbf{E}$ is sufficiently larger than $\mathbf{E}_o$. For $\eta_o \ll 1$, η depends both on F and on η_a. In particular, if $F \gg 1/\eta_o$ the quantum efficiency approaches η_a. In this case, a strong Purcell factor improves the quantum efficiency, which further contributes to the fluorescence enhancement, as shown in equation (1). It is worth mentioning that a faster decay rate also increases the emitter saturation threshold, thus enabling the absorption and emission of more photons per second.

These considerations imply that improving fluorescence with a nanoantenna requires systems that deliver at the same time a strong local electric field $\mathbf{E}$, a large Purcell factor F and an antenna efficiency η_a close to one. While there are many examples of nanostructures that exhibit a strong field enhancement [25]–[33], fewer studies of F and η_a have been reported [8]–[12], [34]–[36]. However, it should be noted that the field intensity enhancement and the

Purcell factor are related to each other by the antenna directivity [37] and for a nanoantenna that does not modify the radiation pattern of the emitter, these two quantities are equal [37, 38]. We have recently shown that gold nanospheroids can increase the radiative decay rate by three orders of magnitude, whereas η_a remains close to one [36]. Here, we present a more detailed study of nanospheroids [9, 10, 27, 33] and compare them with gold nanorods [30, 31, 33, 39]. We focus on the wavelength range between 600 nm and 1100 nm, which covers the emission frequency of several molecules [3, 4, 19, 20] and nanocrystals [14, 15]. Furthermore, we consider only the case where the emitter is placed at and oriented along the longitudinal axis of the nanoparticle [36] and, to investigate an experimentally feasible situation, we set the distance between emitter and nanoparticle to no less than 10 nm.

The paper is organized as follows. In section 2, we briefly describe the approach for the calculation of the decay rates. In section 3, we present and discuss results for single and paired gold nanorods, and for paired gold nanospheroids. In section 4, we draw some conclusions.

2. Computational approach

The decay rates can be obtained using classical electrodynamics if the ratios of the modified rates with respect to the values in vacuum or in a homogeneous background are considered [40]. Because the nanoantenna introduces a certain amount of losses, we have to consider both the radiative Γ_{rad} and the total Γ_{tot} decay rates. We compute these quantities by considering the power emitted by a classical oscillating dipole and normalize it with respect to the case without a nanoantenna.

$$\frac{\Gamma_{rad}}{\Gamma^{o}_{rad}} = \frac{P_{rad}}{P^{o}_{rad}}, \qquad \frac{\Gamma_{tot}}{\Gamma^{o}_{rad}} = \frac{P_{tot}}{P^{o}_{rad}}, \tag{3}$$

where P_{rad} is the power radiated to the far field and P_{tot} is the total power, i.e. including that absorbed by the metal. The superscripts indicate the quantities for an isolated emitter in the same background medium as the nanoantenna. Notice that the normalization of Γ_{tot} is not with respect to $\Gamma^{o}_{tot} = \Gamma^{o}_{rad} + \Gamma^{o}_{nrad}$ because the nanoantenna does not modify the internal nonradiative decay channels, which are responsible for Γ^{o}_{nrad}. In fact the total decay rate is actually $\Gamma_{tot} + \Gamma^{o}_{nrad}$. The quantities in equation (2) are thus given by $F = \Gamma_{rad}/\Gamma^{o}_{rad}$ and $\eta_a = \Gamma_{rad}/\Gamma_{tot}$. P_{rad} and P_{tot} are given by integrating the Poynting vector over two surfaces that contain the dipolar source and the nanoantenna (see figure 1(b)). The inner surface collects the total emitter power, whereas the outer surface collects the radiated power.

Because we consider nanoantennas having dimensions comparable with the effective wavelength of light in the metal [41], we need to take electrodynamic effects fully into account [12]. These quantities can be computed using the finite-difference time-domain (FDTD) method [42]. Since the onset of large electric fields at the nanoparticle surface and the nanoscale geometry require fine meshes for getting accurate results [36], [42]–[44], even if the overall size of the system is small the computational burden becomes considerable. However, since the nanoantenna and the source exhibit rotational symmetry, we can exploit the body of revolution (BOR) technique in the FDTD method [45] to reduce the original three-dimensional (3D) problem to a 2D one (see figure 1). When we deal with very fine meshes, the BOR–FDTD method can significantly decrease the required memory and computation time. This approach has been used in various applications such as modeling wave propagation through optical

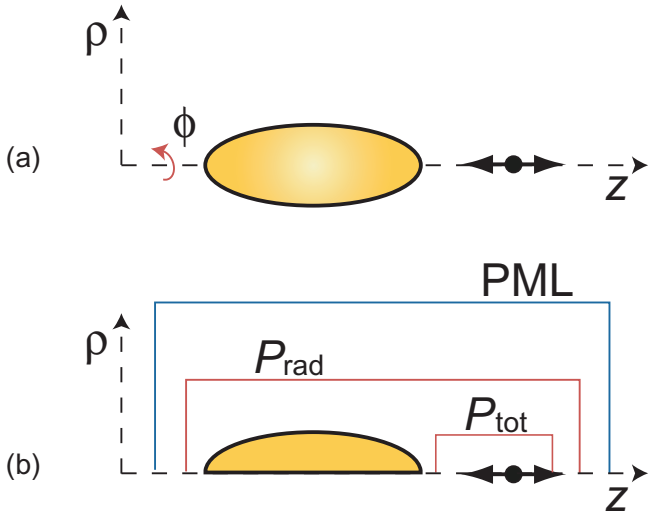

Figure 1. A single emitter is coupled to a nanoantenna. (a) The nanoantenna and the emitter are such that the system forms a BOR. (b) In the BOR–FDTD approach the 3D problem can be reduced to a 2D one by considering only a plane containing the z-axis. The total and radiated powers are computed using the Poynting theorem (red lines). The mesh is truncated using PML absorbing boundary conditions (blue line).

lenses [46], resonant cavities [47], and the calculation of spontaneous emission lifetime in a microcavity [48].

For a rotationally symmetric problem, the electric and magnetic fields in cylindrical coordinates can be expressed as an infinite Fourier-series expansion of the form

$$\mathbf{E}(\rho, \phi, z) = \sum_{m=0}^{\infty} (\mathbf{E}_{\mathrm{e},m}(\rho, z) \cos m\phi + \mathbf{E}_{\mathrm{o},m}(\rho, z) \sin m\phi), \tag{4}$$

$$\mathbf{H}(\rho, \phi, z) = \sum_{m=0}^{\infty} (\mathbf{H}_{\mathrm{e},m}(\rho, z) \cos m\phi + \mathbf{H}_{\mathrm{o},m}(\rho, z) \sin m\phi), \tag{5}$$

where m is the mode number. For isotropic materials, these modes are uncoupled from each other, and their number depends on the excitation symmetry. In our case, where a dipole is located at and directed along the symmetry axis z, only the zeroth-order mode is necessary ($m = 0$). Furthermore, only three electromagnetic-field components are required ($E_{\rho,\mathrm{e},0}$, $E_{z,\mathrm{e},0}$ and $H_{\phi,\mathrm{e},0}$), corresponding to a transverse magnetic mode. As shown in figure 1(b), we employ perfectly-matched-layer (PML) absorbing boundary conditions to truncate the computational domain without introducing spurious reflections [49]. The dielectric function of the gold nanoantenna [50] is modeled as described in [42] by a Drude–Lorentz dispersion model. Moreover, the nanoantenna is embedded in glass ($n_{\mathrm{b}} = 1.5$). In the following we set the mesh pitch to 1 nm. Convergence studies down to 0.5 nm show that the results may change by up to 5% depending on the specific nanoantenna configuration.

3. Results and discussion

3.1. Nanorods

We first consider an emitter coupled to a single gold nanorod, as sketched in the inset of figure 2(a). The emitter is at a fixed orientation and distance $d = 10$ nm from the nanorod, while the nanoparticle aspect ratio and volume change. Moreover, we focus on nanorods that are up to 100 nm long to obtain plasmon resonances in the visible and near-infrared spectral range. Figures 2(a)–(c) show that the plasmon peak redshifts when the nanorod long axis a increases or the nanorod short axis b decreases. Therefore, by tuning the aspect ratio b/a one can easily place the plasmon resonance at the desired spectral location [31, 33]. The Purcell factor is close to 600 for wavelengths around 1000 nm. However, when the resonance shifts toward the visible spectrum, the enhancement rapidly drops to values below 100.

Another important quantity that enters equation (2) is the antenna efficiency η_a. As shown in figures 2(a)–(c), η_a increases with the volume of the nanorod, i.e. as b becomes larger. Unfortunately, the largest Purcell factors correspond to the lowest efficiencies because a higher aspect ratio implies a reduced volume. Interestingly, for this system the antenna efficiency is not smaller at the plasmon resonance as predicted for a nanosphere [34] and an SNOM tip [35]. Instead, as one can see by comparison of figure 2(a) with figure 2(c), when the resonance moves toward shorter wavelengths, η_a gets larger. This happens despite the fact that material losses in the nanoparticle increase in going to higher frequencies [50], showing that the plasmon resonance plays a fundamental role in keeping the antenna efficiency high. In summary, a single gold nanorod cannot establish a very large Purcell factor and a high η_a at the same time, when the emitter is at least 10 nm away from the nanoantenna.

Because we have chosen to fix d to 10 nm in this work, we now explore other solutions for achieving better performance. A straightforward approach is to place the emitter between two nanorods, each 10 nm away from it, as shown in the inset of figure 3(c). The Purcell factor now reaches values up to 3000, but it quickly falls as the aspect ratio decreases. Moreover, because the interaction between the two nanorods redshifts the plasmon resonance, obtaining a strong enhancement at wavelengths below 750 nm has become more difficult. The shift of the plasmon resonance manifests itself also in η_a, which increases with the wavelength slightly less rapidly than in figure 2, but it reaches a higher plateau [36]. Furthermore, like for the case of a single nanorod, the largest Purcell factors occur with the lowest antenna efficiencies.

In figures 2 and 3, the steep decrease of the Purcell factor in reducing the aspect ratio comes from the fact that the head of the nanorods is flat. Thus the localized field enhancement is rapidly lost when the nanorod gets thicker. To avoid this issue we consider nanorods with rounded ends, presented in figure 4. In comparing figure 3(b) with figure 4, we notice three important aspects. Firstly, for high aspect ratios the rounded nanorods exhibit smaller Purcell factors, while the antenna efficiency remains almost the same. Secondly, for low aspect ratios these nanorods lose their Purcell enhancement slightly more slowly than the flat ones, but the redshift of the resonance peak is much weaker. Consequently, finding a structure that has a strong enhancement at shorter wavelengths is easier. Thirdly, the antenna efficiency reaches its plateau already at wavelengths close to 650 nm if the aspect ratio is less than 2. Thus, for the parameters considered here, rounding the nanorod ends is advantageous for getting large Purcell factors near the visible range, whereas at large aspect ratios flat ends yield a better enhancement.

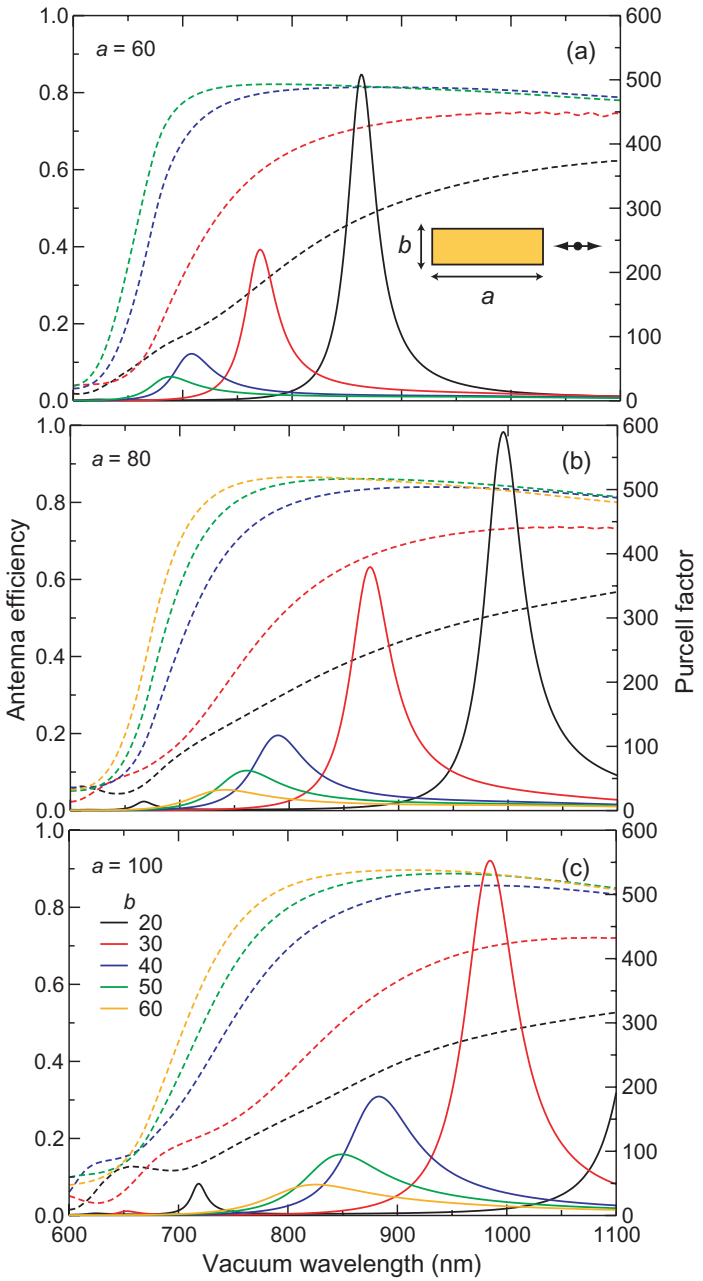

Figure 2. (a)–(c) Antenna efficiency η_a (dashed curves) and Purcell factor F (solid curves) for an emitter coupled to a gold nanorod for various aspect ratios and volumes. The inset in (a) shows the position and orientation of the emitter with respect to the nanorod. The nanorod dimensions a and b are given in nanometres. The emitter is at a fixed distance $d = 10$ nm from the nanorod.

To emphasize these aspects, in figure 5 we compare the two systems as a function of the particle length a, while keeping the width b fixed. For $a = 80$ the nanorods with rounded ends exhibit a slightly stronger Purcell factor than those with flat ends, and the peak is shifted by nearly 150 nm toward the visible range.

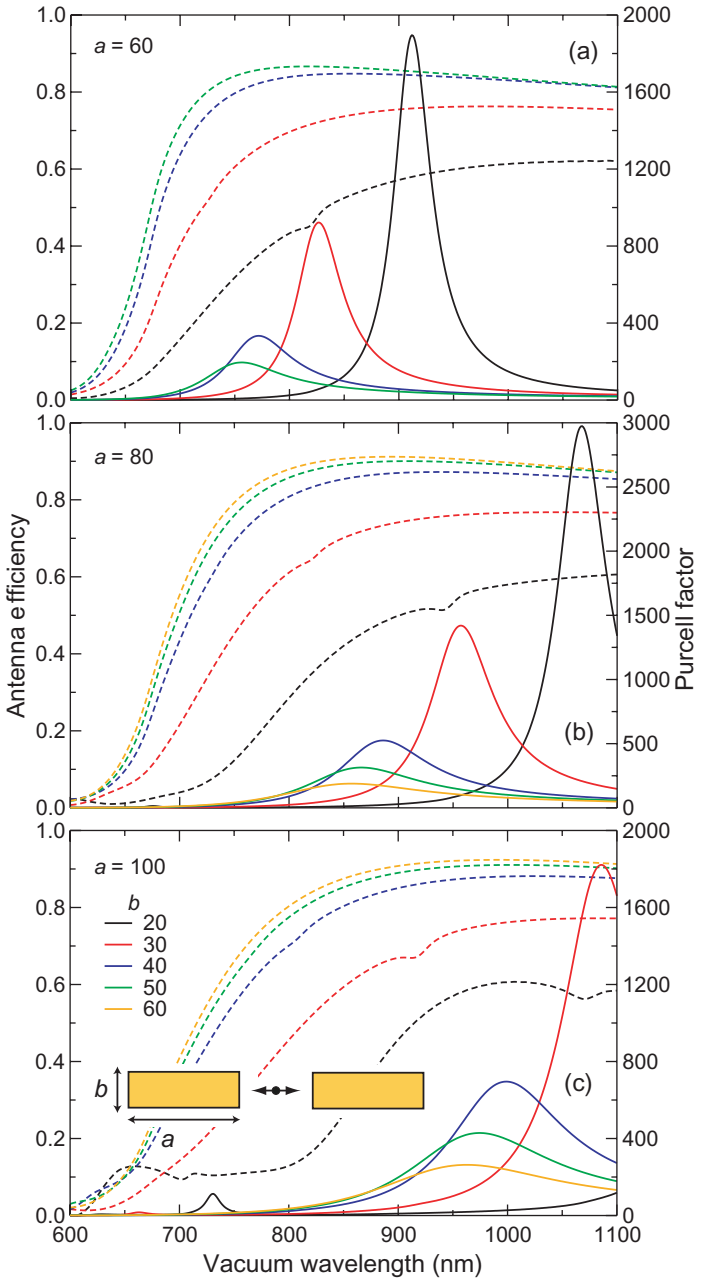

Figure 3. (a)–(c) Antenna efficiency η_a (dashed curves) and Purcell factor F (solid curves) for an emitter coupled to two gold nanorods for various aspect ratios and volumes. The inset in (c) shows the position and orientation of the emitter with respect to the nanorods. The nanorod dimensions a and b are given in nanometres. The emitter is centered at a fixed distance $d = 10$ nm from both nanorods.

3.2. Nanospheroids

In the previous section, we have seen that in the chosen spectral range nanorods can lead to large enhancements only for high aspect ratios, which unfortunately correspond also to

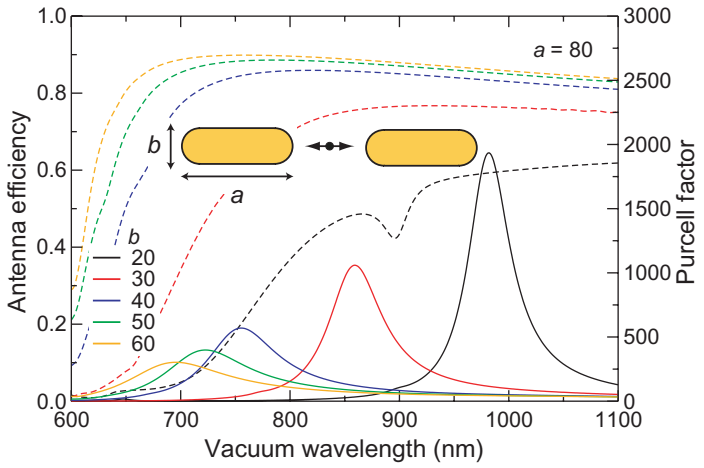

Figure 4. Antenna efficiency η_a (dashed curves) and Purcell factor F (solid curves) for an emitter coupled to two rounded gold nanorods for various aspect ratios and volumes. The inset shows the position and orientation of the emitter with respect to the nanorods. The nanorod dimensions a and b are given in nanometres. The emitter is centered at a fixed distance $d = 10$ nm from both nanorods. The nanorods have ends rounded by a hemisphere.

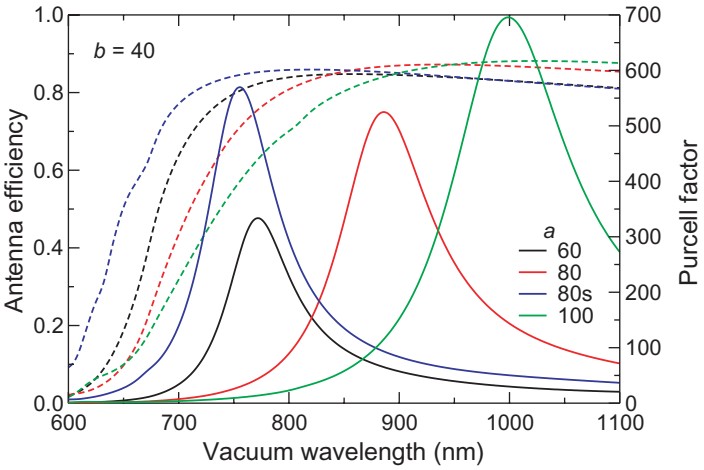

Figure 5. Antenna efficiency η_a (dashed curves) and Purcell factor F (solid curves) for an emitter coupled to two gold nanorods of various aspect ratios and volumes. The emitter position and the nanorod parameters are as given in figure 3 ($a = 60$–100 nm) and figure 4 ($a = 80$ nm, indicated as 80 s in the legend).

lower antenna efficiencies. By rounding the nanorod ends the Purcell factor remains higher for smaller aspect ratios, where η_a is closer to one. To improve the enhancement, next we consider nanospheroids [9, 10, 27, 33, 36], which have similar geometrical parameters but sharper ends than nanorods. Figures 6(a)–(c) present the Purcell factor and η_a for various aspect ratios and volumes of the nanoparticles. Compared to nanorods the enhancement is larger at

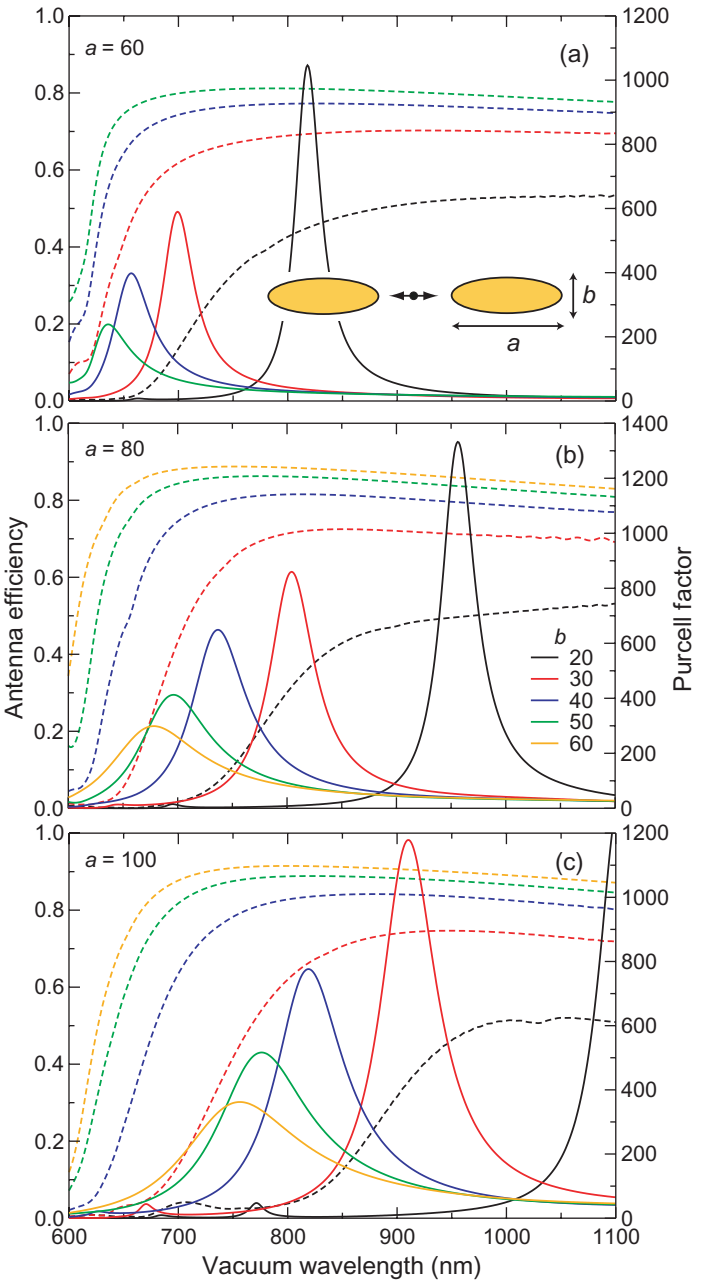

Figure 6. (a)–(c) Antenna efficiency η_a (dashed curves) and Purcell factor F (solid curves) for an emitter coupled to two gold nanospheroids for various aspect ratios and volumes. The inset in (a) shows the position and orientation of the emitter with respect to the nanospheroids. The nanospheroid dimensions a and b are given in nanometres. The emitter is centered at a fixed distance $d = 10$ nm from both nanospheroids.

shorter wavelengths because the reduced aspect ratio is partially compensated by a sharper rounding of the nanoparticle ends. Therefore, we conclude that nanospheroids perform better than nanorods in the spectral range between 600 and 900 nm if both the Purcell factor and the antenna efficiency have to be optimized.

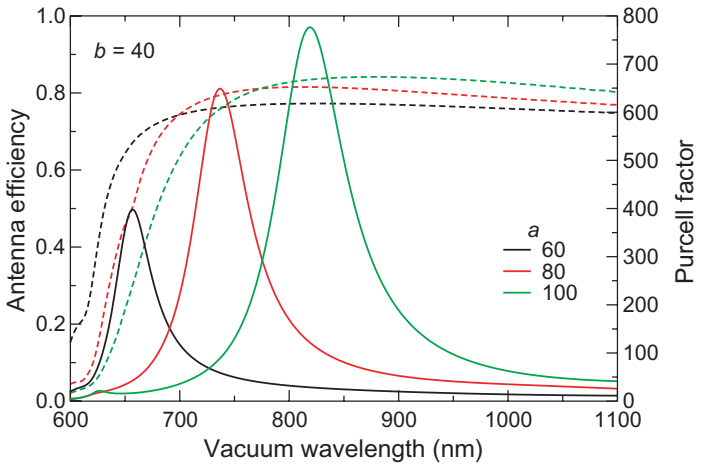

Figure 7. Antenna efficiency η_a (dashed curves) and Purcell factor F (solid curves) for an emitter coupled to two gold nanospheroids of various aspect ratios and volumes. The emitter position and the nanospheroid parameters are as given in figure 6 ($a = 60$–100 nm).

In figure 7, we focus on a selection of the data from figure 6, where the nanoparticle width b is fixed to be 40 nm, whereas the length a changes from 60 to 100 nm. The results show that a large Purcell factor together with a high antenna efficiency are achieved for shorter wavelengths than for the nanorods discussed in figure 5. In particular, notice the enhancement of about 400 with an antenna efficiency of 70% obtained at wavelengths as short as 650 nm.

These results have been obtained assuming that the emitter is fixed at a distance of 10 nm from the nanoparticles. However, it is well known that the enhancement rapidly falls off when the distance increases [8, 36]. Figure 8 displays the effect for the system under study and for selected dimensions ($a = 100$ nm and $b = 40$ nm). Here, the distance varies from both nanoparticles, such that $d = 20$ nm corresponds to two nanospheroids separated by 40 nm with the emitter at the center of the gap. Despite the reduced enhancement, the Purcell factor is still more than 100 for $d = 20$ nm. On the other hand, the antenna efficiency does not change much, suggesting that the emitter can be still placed closer to the nanoparticle without a significant increase of losses [36]. The inset in figure 8 represents a snapshot of the electric field generated by the emitter acting as a dipolar source. The wavelength is on resonance and the emitter is at a distance $d = 10$ nm from the nanospheroids. The plot illustrates that the enhancement drops with distance because the near field of the dipolar source is strongly confined. In particular, because it decays more rapidly than the near field of the nanoparticles, it turns out that the best position for the emitter is not at the center of the nanoantenna gap. Figure 9 explains this concept for the case where the nanospheroids are separated by 30 nm and the emitter is displaced 1 to 5 nm along the nanoparticle axis away from the center. The Purcell factor gets larger as the emitter approaches one nanoparticle. Notice that as the system becomes asymmetric, the excitation of a higher order resonance at 750 nm becomes noticeable. This is not a serious issue, because the emitter has a much narrower linewidth than the plasmon resonance. However, we have to keep in mind that the displacement also affects the emission pattern [4, 23, 36, 51], [52]–[54], as shown in the inset of figure 9, and the polarization [55]. These effects are even stronger for

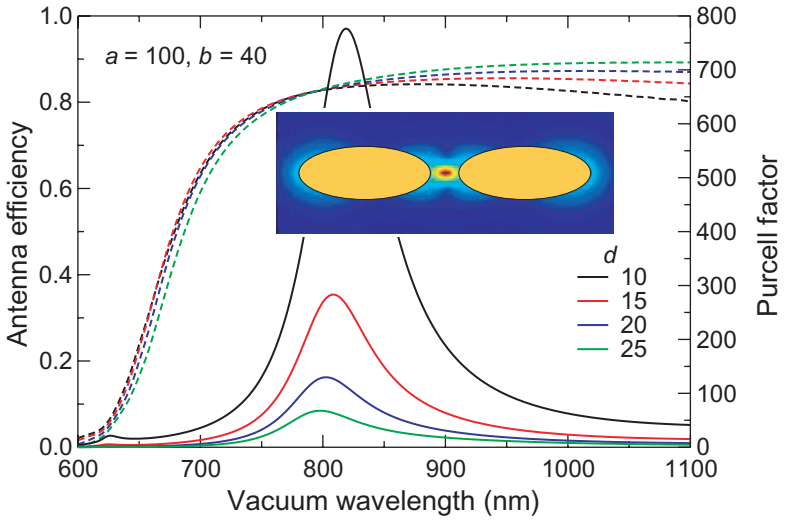

Figure 8. Antenna efficiency η_a (dashed curves) and Purcell factor F (solid curves) for an emitter coupled to two gold nanospheroids for various distances $d = 10$–25 nm from both nanoparticles. The emitter position and the nanospheroid parameters are as given in figure 6 ($a = 100$ nm and $b = 40$ nm). The inset displays a snapshot of the electric field (log10 scale) at the plasmon resonance for $d = 10$ nm.

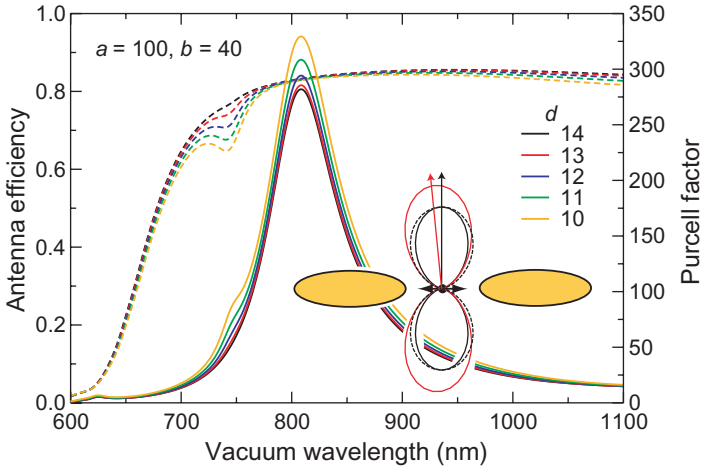

Figure 9. Antenna efficiency η_a (dashed curves) and Purcell factor F (solid curves) for an emitter coupled to two gold nanospheroids separated by 30 nm for various distances $d = 10$–14 nm from one of the two nanoparticles. The emitter orientation and the nanospheroid parameters are given as in figure 6 ($a = 100$ nm and $b = 40$ nm). The inset plots the far-field emission pattern at the plasmon resonance for $d = 10$ nm (red curve), $d = 15$ nm (black curve) and an isolated emitter (dashed curve). The latter is rescaled for better comparison with the previous two cases. The dipole is shifted to the right and the arrows indicate the direction of maximal radiation.

smaller antenna gaps and shorter distances (not shown here). We point out that also for an emitter coupled to a single nanoparticle the emission pattern is modified [12, 23, 51, 54]. The inset of figure 9 also shows the far-field profile of an isolated dipole (dashed curve) to stress the fact that even when the emitter is at the center of the nanoantenna gap its radiation pattern has changed (see the black curve). Therefore, the Purcell factor and the field intensity enhancement are similar, but not equal [37]. Moreover, because the antenna directivity is also wavelength-dependent, these two quantities cannot be matched by simply applying a scaling factor. However, since the deviation from dipolar emission is small, our results on the Purcell factor are also applicable to the field enhancement at the emitter position and they are thus related to previous work [27, 31, 33].

4. Conclusions

We have used the BOR–FDTD method to calculate the decay rates of an emitter coupled to a gold nanoantenna. Although the model is limited to emitters located and oriented such that the system preserves cylindrical symmetry, BOR–FDTD allows the study of several systems with the computational burden and speed of a 2D FDTD calculation. We have considered single and paired nanorods as well as paired nanospheroids. In the spectral range between 600 and 900 nm, we have found that nanospheroids exhibit a better performance than nanorods in terms of Purcell factor F and antenna efficiency η_a. The reason for this is that they are sharper than nanorods when the aspect ratio is small. We also find that the enhancement is larger if the emitter is closer to one of the two nanoparticles, rather than being at the center. Such a symmetry breaking also implies a modification of the emission pattern. Choosing a different background index will cause a spectral shift of the antenna resonance, but the general findings remain valid. These results highlight the fact that experiments require great control over the emitter position, especially if large enhancements are desired. Mastering these properties in the laboratory will make gold nanospheroids very attractive for applications in field-enhanced spectroscopy, optoelectronics and active metamaterials at visible and near-infrared frequencies.

Acknowledgments

We thank L Rogobete, F Kaminski, N Mojarad, H Eghlidi and S Götzinger for helpful discussions. A Mohammadi is grateful to the Persian Gulf University Research Council for partial support. This work was financed by the ETH Zurich initiative on Composite Doped Metamaterials (CDM).

References

[1] Metiu H 1984 *Prog. Surf. Sci.* **17** 153
[2] Moskovits M 1985 *Rev. Mod. Phys.* **57** 783
[3] Anger P, Bharadway P and Novotny L 2006 *Phys. Rev. Lett.* **96** 113002
[4] Kühn S, Håkanson U, Rogobete L and Sandoghdar V 2006 *Phys. Rev. Lett.* **97** 017402
[5] Greffet J-J 2005 *Science* **308** 1561

[6] Bohren C F and Huffman D R 1983 *Absorption and Scattering of Light by Small Particles* (New York: Wiley)
[7] Chance R R, Prock A and Silbey R 1978 *Adv. Chem. Phys.* **37** 1
[8] Ruppin R 1982 *J. Chem. Phys.* **76** 1681
[9] Gersten J and Nitzan A 1981 *J. Chem. Phys.* **75** 1139
[10] Klimov V V, Ducloy M and Letokhov V S 2002 *Eur. Phys. J.* D **20** 133
[11] Blanco L A and García de Abajo F J 2004 *Phys. Rev.* B **69** 205414
[12] Mertens H, Koenderink A F and Polman A 2007 *Phys. Rev.* B **76** 115123
[13] Alù A and Engheta N 2008 *Phys. Rev. Lett.* **101** 043901
[14] Farahani J N, Pohl D W, Eisler H J and Hecht B 2005 *Phys. Rev. Lett.* **95** 017402
[15] Biteen J S, Pacifici D, Lewis N S and Atwater H A 2005 *Nano Lett.* **5** 1768
[16] Mertens H and Polman A 2006 *Appl. Phys. Lett.* **89** 211107
[17] Taminiau T H, Moerland R J, Segerink F B, Kuipers L and van Hulst N F 2007 *Nano Lett.* **7** 28
[18] Tam F, Goodrich G P, Johnson B R and Halas N J 2007 *Nano Lett.* **7** 496
[19] Zhang J, Fu Y, Chowdhury M H and Lakowicz J R 2007 *Nano Lett.* **7** 2101
[20] Bakker R M, Yuan H-K, Liu Z, Drachev V P, Kildishev A V, Shalaev V M, Pedersen R H, Gresillon S and Boltasseva A 2008 *Appl. Phys. Lett.* **92** 043101
[21] Chang D E, Sørensen A S, Hemmer P R and Lukin M D 2006 *Phys. Rev. Lett.* **97** 053002
[22] Chang D E, Sørensen A S, Hemmer P R and Lukin M D 2007 *Phys. Rev.* B **76** 035420
[23] Kühn S, Mori G, Agio M and Sandoghdar V 2008 *Mol. Phys.* **106** 893
[24] Agio M *et al* 2007 *Proc. SPIE* **6717** 67170R
[25] Aravind P K, Niztan A and Metiu H 1981 *Surf. Sci.* **110** 189
[26] Kottman J P, Martin O J F, Smith D R and Schultz S 2001 *Chem. Phys. Lett.* **341** 1
[27] Calander N and Willander M 2002 *J. Appl. Phys.* **92** 4878
[28] Hao E and Schatz G C 2003 *J. Chem. Phys.* **120** 357
[29] Aizpurua J, Hanarp P, Sutherland D S, Käll M, Bryant G W and García de Abajo F J 2003 *Phys. Rev. Lett.* **90** 057401
[30] Mühlschlegel P, Eisler H-J, Martin O J F, Hecht B and Pohl D W 2005 *Science* **308** 1607
[31] Aizpurua J, Bryant G W, Richter L J, García de Abajo F J, Kelley B K and Mallouk T 2005 *Phys. Rev.* B **71** 235420
[32] Sundaramurthy A, Crozier K B, Kino G S, Fromm D P, Schuck P J and Moerner W E 2005 *Phys. Rev.* B **72** 165409
[33] Liu M, Guyot-Sionnest P, Lee T-W and Gray S K 2007 *Phys. Rev.* B **76** 235428
[34] Thomas M, Greffet J-J, Carminati R and Arias-Gonzalez J R 2004 *Appl. Phys. Lett.* **85** 3863
[35] Carminati R, Greffet J-J, Henkel C and Vigoureux J M 2006 *Opt. Commun.* **261** 368
[36] Rogobete L, Kaminski F, Agio M and Sandoghdar V 2007 *Opt. Lett.* **32** 1623
[37] Taminiau T H, Stafani F D and van Hulst N F 2008 *Opt. Express* **16** 10858
[38] Biteen J S, Sweatlock L A, Mertens H, Lewis N S, Polman A and Atwater H A 2007 *J. Phys. Chem.* C **111** 13372
[39] Sönnichsen C, Franzl T, Wilk T, von Plessen G, Feldmann J, Wilson O and Mulvaney P 2002 *Phys. Rev. Lett.* **88** 077402
[40] Xu Y, Lee K and Yariv A 2000 *Phys. Rev.* A **61** 033807
[41] Novotny L 2007 *Phys. Rev. Lett.* **98** 266802
[42] Kaminski F, Sandoghdar V and Agio M 2007 *J. Comput. Theor. Nanosci.* **4** 635
[43] Oubre C and Nordlander P 2004 *J. Phys. Chem.* B **108** 17740
[44] Mohammadi A, Jalali T and Agio M 2008 *Opt. Express* **16** 7397
[45] Taflove A and Hagness S C 2005 *Computational Electrodynamics: the Finite-Difference Time-Domain Method* (Norwood, MA: Artech House)
[46] Davidson D and Ziolkowski R 1994 *J. Opt. Soc. Am.* A **11** 1471
[47] Chen Y, Mittra R and Harms P 1996 *IEEE Trans. Microw. Theory Tech.* **44** 832

[48] Xu Y *et al* 1993 *J. Opt. Soc. Am.* B **16** 465
[49] Prather D W and Shi S 1999 *J. Opt. Soc. Am.* A **16** 1131
[50] Lide D R (ed) 2006 *CRC Handbook of Chemistry and Physics* 87th edn (Boca Raton, FL: CRC Press)
[51] Rogobete L 2007 The influence of the nano-environment on the optical properties of a dipole emitter a theoretical study *Dissertation ETH No. 16813* (ETH, Zurich, Switzerland)
[52] Hofmann H F, Kosako T and Kayoda Y 2007 *New J. Phys.* **9** 217
[53] Li J, Salandrino A and Engheta N 2007 *Phys. Rev.* B **76** 245403
[54] Taminiau T H, Stefani F D, Segerink F B and van Hulst N F 2008 *Nat. Photonics* **2** 234
[55] Moerland R J, Taminiau T H, Novotny L, van Hulst N F and Kuipers L 2008 *Nano Lett.* **8** 606